ADVANCING EARTH AND SPACE SCIENCES

Geophysical Research Letters

RESEARCH LETTER
10.1029/2024GL113672

Timing of the Recent Migration and Intensification of the Southern Hemisphere Westerly Winds

Dieter R. Tetzner[1], **Claire S. Allen**[1], **Elizabeth R. Thomas**[1], **Eric W. Wolff**[2], and **Christian L. E. Franzke**[3]

[1]British Antarctic Survey, Ice Dynamics and Paleoclimate, Cambridge, UK, [2]Department of Earth Sciences, University of Cambridge, Cambridge, UK, [3]Center for Climate Physics, Institute for Basic Science, Busan, South Korea

Key Points:

- Southern Hemisphere Westerly wind reconstruction shows a clear trend since the 1960s, unprecedented in the context of the past 140 years
- The 1960s wind shift and acceleration is coincident with anthropogenically induced increase in greenhouse gases and ozone depletion

Supporting Information:

Supporting Information may be found in the online version of this article.

Correspondence to:

D. R. Tetzner,
dietet95@bas.ac.uk

Citation:

Tetzner, D. R., Allen, C. S., Thomas, E. R., Wolff, E. W., & Franzke, C. L. E. (2025). Timing of the recent migration and intensification of the Southern Hemisphere westerly winds. *Geophysical Research Letters*, *52*, e2024GL113672. https://doi.org/10.1029/2024GL113672

Received 2 DEC 2024
Accepted 19 JUN 2025

Author Contributions:

Conceptualization: Dieter R. Tetzner, Claire S. Allen, Elizabeth R. Thomas, Eric W. Wolff
Data curation: Dieter R. Tetzner
Formal analysis: Dieter R. Tetzner, Christian L. E. Franzke
Investigation: Dieter R. Tetzner, Claire S. Allen, Elizabeth R. Thomas
Methodology: Dieter R. Tetzner, Claire S. Allen
Supervision: Claire S. Allen, Elizabeth R. Thomas, Eric W. Wolff
Validation: Claire S. Allen
Visualization: Dieter R. Tetzner, Claire S. Allen
Writing – original draft: Dieter R. Tetzner
Writing – review & editing: Claire S. Allen, Elizabeth R. Thomas, Eric W. Wolff, Christian L. E. Franzke

Abstract In recent decades, the Southern Hemisphere westerly winds have strengthened and migrated south, attributed to greenhouse gas emissions and stratospheric ozone depletion. However, the onset and acceleration of these drivers is coincident with the start of the instrumental record, thus, hindering our ability to determine the significance of the recent trends. Here, we present a novel wind reconstruction based on marine diatoms preserved in an Antarctic Peninsula ice core, providing a unique record to reconstruct westerly winds across the Pacific sector of the Southern Ocean (SO). The annually resolved record provides clear evidence that a southward migration of the Pacific sector westerly wind belt occurred in the 1960s, coupled with a prolonged strengthening trend. The poleward shift and acceleration of the westerly winds across this SO sector is unprecedented in the context of the past 140 years and coincident with the anthropogenically induced increase in greenhouse gases and ozone depletion.

Plain Language Summary The Southern Hemisphere Westerly winds are a key component of the Earth's climate system, driving ocean circulation and changes in the Antarctic ice sheet that directly impact global sea levels. In recent years, these winds have become stronger and moved south, likely due to greenhouse gas emissions and ozone depletion. In this study we reconstructed past westerly wind variability in the Pacific sector of the Southern Ocean using Antarctic ice core samples and found that the southward shift began in the 1960s, accompanied by a long-term strengthening of the winds. This change is unprecedented over the last 140 years and likely related to human activities.

1. Introduction

The Southern Hemisphere Westerly Winds (SHWW) play a crucial role in the global climate system by modulating the upwelling of carbon-rich, and relatively warm, deep water in the Southern Ocean (SO) (Dutrieux et al., 2014; Gille, 2014; Gruber et al., 2019; Landschützer et al., 2015; Le Quéré et al., 2018; Thoma et al., 2008). Variations in the SHWW are represented by the Southern Annular Mode (SAM) (Marshall, 2003), which has exhibited a positive trend since observations began, characterized by the strengthening and southward migration of the SHWW belt (Fogt & Marshall, 2020; Marshall, 2003). The shift to more southerly and stronger SHWW is considered among the main drivers of observed environmental changes in the Antarctic Peninsula (AP) and West Antarctica. These include: (a) reduced sea ice cover in the Bellingshausen Sea sector (Parkinson, 2019); (b) higher snow accumulation (Thomas et al., 2008; Van Wessem et al., 2016); (c) widespread warming (Steig et al., 2009; Turner et al., 2020); and (d) accelerated melting of ice shelves and tidewater glaciers along the coastline of the Amundsen-Bellingshausen Seas (Pritchard et al., 2012), most of them ultimately contributing to global mean sea-level rise (Shepherd et al., 2012; Vaughan, 2006).

It is widely believed these changes in SHWW have occurred in response to the increased greenhouse gas (GHG) concentrations in the troposphere and stratospheric ozone depletion (Arblaster & Meehl, 2006; Franzke et al., 2015; Thompson et al., 2011; D. W. J. Thompson and Solomon, 2002). However, the onset of ozone depletion and the acceleration of GHG warming coincide with the time when multiple permanent meteorological stations at 40° and 65°S began measuring atmospheric parameters (hereafter instrumental period (1958 CE-present)) (Marshall, 2003). Therefore, our understanding of the long-term shifts and influence of the SHWW belt is limited by the short and sparse observational records. Numerous paleoclimate archives (e.g., marine sediments, lake sediments, peat-bogs, speleothems, ice cores) throughout the Southern Hemisphere have been utilized to reconstruct past SHWW, but many are limited by their reliance on precipitation or temperature proxies to infer SHWW changes (Browne et al., 2017; Hinojosa et al., 2017; Koffman et al., 2014; Laluraj

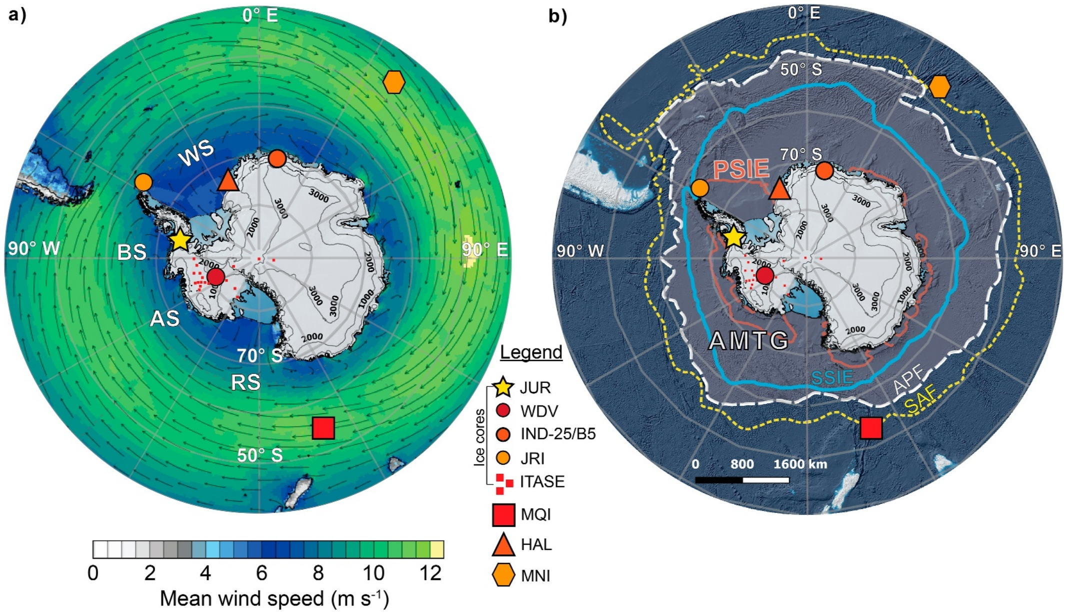

Figure 1. Maps showing the location of the Jurassic ice core (JUR; yellow star) and other records included in this study (red and orange colored symbols). (a) The JUR site in relation to the Southern Hemisphere Westerly Winds belt. Arrows in (a) represent the direction of sea surface-level winds (10 m). Colors in (a) represent the annual sea surface-level (10 m) wind speed from ERA5 between 1979 and 2012. (b) The JUR site in relation to oceanographic zones around Antarctica. Gray shaded area in (b) represents the source region of the Antarctic marine taxa group. WS = Weddell Sea, BS = Bellingshausen Sea, AS = Amundsen Sea, RS = Ross Sea, PSIE = Perennial Sea Ice Edge, SSIE = Seasonal Sea Ice Edge, APF = Antarctic Polar Front, SAF = Sub-Antarctic Front, MNI = Marion Island, MQI = Macquarie Island, WDV = WAIS Divide (Koffman et al., 2014), JRI = James Ross Island (McConnell et al., 2007). ITASE = International Trans-Antarctic Scientific Expedition (Dixon et al., 2012). IND-25/B5 = ice core (Laluraj et al., 2020). HAL = Halley Research Station.

et al., 2020; McConnell et al., 2007; Moreno et al., 2014; Moy et al., 2008; Schimpf et al., 2011; Waldmann et al., 2010; Xia et al., 2018), or coarse temporal resolution (Browne et al., 2017; Moy et al., 2008; Waldmann et al., 2010). While some recent studies have made considerable improvements to the resolution and employed novel wind proxies (Perren et al., 2020; Saunders et al., 2018), all are based on the interaction of winds with fixed locations. Thus, we cannot unequivocally differentiate between past wind strength and migration of the wind belt. This limitation has prevented us from establishing whether the core of the westerly wind belt was already migrating and/or strengthening by the time GHGs changed and ozone depletion occurred. Not knowing the timing of SHWW changes limits our understanding of the causes of westerly wind variations and the roles they play in driving recent environmental changes in Antarctica. The diatom records preserved in ice cores have the potential to resolve the timing of SHWW migration and strengthening.

Diatoms, microscopic unicellular algae, inhabit aquatic environments worldwide (Smol and Stoermer, 2010). Diatoms can be lifted from the sea-surface microlayer into the atmosphere by wind-induced bubble-bursting and wave-breaking processes (Cipriano & Blanchard, 1981; Farmer et al., 1993), transported by winds over long distances (Elster et al., 2007; Harper & McKay, 2010), and deposited over the Antarctic ice sheet (Budgeon et al., 2012) where they can get buried by subsequent snowfall events. Recently, the diatom content of ice cores from high-elevation inland sites in the southern AP has been shown to record key information about the variability of SHWW, with no evident biases caused by preferential deposition, seasonality or sea ice dynamics (Allen et al., 2020; D. R. Tetzner, Thomas, et al., 2022; D. R. Tetzner, Allen, & Thomas, 2022). This new proxy has been tested at multiple sites in the region, providing a robust proxy for wind conditions in the Pacific sector of the SHWW belt during the satellite-era (1979 CE-present) (Allen et al., 2020; D. R. Tetzner, Thomas, et al., 2022). Here we present the first detailed study of an extended annually-resolved diatom record, spanning the past 140 years from the Jurassic ice core in the southern AP (Figure 1). We analyze the variability in the annual diatom assemblage and abundance to reconstruct latitudinal shifts and changes in wind strength in the Pacific core of the SHWW belt (hereafter Pacific SHWW).

2. Methods

2.1. Ice Core Drilling Site and Age Scale

The Jurassic ice core (JUR) was drilled in the austral summer 2012/2013 CE to a depth of 140 m using the British Antarctic Survey (BAS) electromechanical, 104 mm diameter drill. The JUR site is located on an ice plateau in the south-western side of the AP (74.33°S, 73.06°W, 1,139 m a.s.l.), 40 km northwest of a local ice divide, 140 km (>1,000 km) south of the austral summer (winter) sea ice edge (Figure 1b). The absence of topographic barriers between the JUR site and the coastline directly exposes the JUR site to airmasses transported from the Amundsen-Bellingshausen Seas. An ice chronology was established for this core based on the annual cycles of hydrogen peroxide (H_2O_2) and the non-sea salt component of sulfate ($nssSO_4{}^{2-}$). The ice chronology was corroborated using major enhancements in the $nssSO_4{}^{2-}$ signal caused by two large volcanic eruptions, Krakatoa (1883 CE) and Pinatubo (1991 CE) (Cole-Dai et al., 1997; Emanuelsson et al., 2022). The estimated dating error was <±7 months for each year and with no accumulated error.

2.2. Sample Preparation and Analyses

Ice core samples were cut using a band-saw with a steel blade. Discrete samples were cut from the inner part of the ice core at annual resolution for diatom analyses (~6 cm^2 basal area and to the depth equivalent of each year). Ice samples for diatoms analyses were melted and then meltwater was filtered through polycarbonate membrane filters (pore diameter 1.0 μm). Filters were subsequently scanned in a Scanning Electron Microscope (SEM), following the method and constraints presented in D. Tetzner et al. (2021), D. R. Tetzner, Allen, Thomas, et al. (2025).

Diatom identification and ecological associations were based on published SO databases and references therein (Armand et al., 2005; Cefarelli et al., 2010; Hasle & Syvertsen, 1997; Zielinski & Gersonde, 1997). Observations of diatom preservation were based on the visual recognition of characteristic frustule dissolution and degradation features (Warnock & Scherer, 2015). Diatom frustules and fragments with a long axis less than 5 μm were excluded from counting and identification. Diatom counts per sample integrated all diatom valves, partially obscured diatom valves, and fragments with diatom ornamentation identified in each sample. Diatoms were first identified to species level where possible. Diatoms that were impossible to identify unequivocally due to image resolution were combined in genera/morphological groups. Among the reasons preventing the classification of diatoms were the occurrence of valves partly obscured by insoluble particles lying on top, fragments with undiagnostic features, and poorly ornamented or indistinctive fragments. The unclassified diatoms were omitted from assemblage composition and ecological associations but were included in the total diatom counts. The diatom record is presented as counts per sample (n), with each sample representing a year. The diatom abundance parameter includes all diatoms and diatom remains identified on each sample, regardless of their potential source.

The main diatom assemblage composition was established from the identified species and groups with abundances higher than 2.0% of the whole assemblage. Ecological associations were determined for the most abundant species/groups. Based on ecological associations, diatoms were classified into two groups differentiated by their Antarctic endemism (Armand et al., 2005; Cefarelli et al., 2010; Hasle & Syvertsen, 1997; Zielinski & Gersonde, 1997).

2.3. Statistical Treatment and Analyses

The JUR diatom abundance record presented a log-normal distribution; therefore, data treatment and calculations were performed using log-normal statistics. Once in the log-domain, the median and standard deviation were calculated and used to define an outlier threshold. All values exceeding the average by two times the standard deviation were considered outliers and not included for further calculations.

Changepoint analyses were performed on the JUR annual diatom abundance time series to identify the time when the root-mean-square level of the power spectral density signal presented the most significant change. Changepoint calculations were conducted using a 10-year window with nine overlapping data points (Killick et al., 2012). Changepoint calculations were conducted using the "findchangepts" function in Matlab software (MathWorks Inc, 2020).

Trends in the JUR diatom abundance record were identified using the empirical mode decomposition approach (Franzke, 2009; Huang et al., 1998; Huang & Wu, 2008). EMD is an algorithm which decomposes a time series into a finite number of intrinsic mode functions and a nonlinear trend component. The statistical significance of the nonlinear trend is estimated using the Monte Carlo approach (Franzke, 2009).

2.4. Climate Analyses

Monthly reanalysis fields from the fifth generation of the European Center for Medium-Range Weather Forecasts (ECMWF), ERA5 (Hersbach & Dee, 2016), were used to obtain spatial correlations between the JUR diatom abundance and annual means of atmospheric circulation parameters (Mean sea level pressure, 10 m wind speed). Spatial correlations were calculated over the satellite-era.

The Amundsen Sea Low (ASL) Actual Central Pressure Index (Hosking et al., 2013), which defines the atmospheric pressure at the ASL location, was used to calculate the correlation between the annual mean ASL strength and the JUR diatom abundance over the satellite-era.

3. Results

3.1. Environmental Correlations (1979–2012 CE)

Spatial correlation analyses revealed wide regions of statistically significant correlations ($-0.3 < R$ or $R > 0.3$, $p < 0.1$) between the JUR diatom abundance record and atmospheric parameters (mean sea level pressure and wind speed) during the satellite-era. The JUR diatom abundance record is positively correlated with the mean annual wind speed in the Pacific SHWW, centered at the northern limit of the Ross-Amundsen Seas (~120°W–150°E, ~50–60°S) ($R \leq 0.56$, $p < 0.01$) (Figure 2a). The JUR diatom abundance record is negatively correlated with the Mean Sea Level Pressure across the Ross-Amundsen-Bellingshausen Seas ($-0.4 \leq R$, $p < 0.1$). A weak but not statistically significant correlation ($p > 0.1$) was observed between the JUR diatom abundance record and the ASL Pressure Center ($R = -0.26$).

3.2. The JUR Diatom Record (1873–2012 CE)

A total of 4,530 diatom valves and fragments were found in the JUR between 1873 and 2012 CE. Diatoms were well-preserved down-core, with no evidence of dissolution in their structures and delicate ornamentation still present. Diatom colonies (linked chains of individual diatoms) were found along the whole core (deepest recovery of colony from the 1879 CE layer). No clear trend or transition was identified in the proportion of fragments relative to whole diatom frustules down-core.

The total annual diatom abundance presented a mean value of 30.2 ± 17.3 diatoms (139.8 diatoms L^{-1}) (Figure 2b). The total annual diatom abundance exhibited a statistically significant ($p < 0.05$) nonlinear positive trend over the whole record. Changepoint analyses revealed the total annual diatom abundance time series exhibited two periods: (I) comparatively lower diatom abundance and variability (27.5 ± 14.4 diatoms) between 1873 and 1964 CE; and (II) comparatively higher diatom abundance and variability (35.8 ± 21.3 diatoms) after 1965 CE. Period (II) exhibits a statistically significant ($p < 0.01$) linear positive trend of 1 diatom yr^{-1}.

Of the total diatoms counted, 2,319 were identified to genus level or higher. Diatom ecological associations can be used to split the assemblage into an Antarctic Marine Taxa Group (AMTG; 27.46% of the main diatom assemblage) and a Combined Taxa Group (CTG; 72.54% of the main diatom assemblage) (Table S1 in Supporting Information S1). The AMTG includes diatom species that are endemic and regular components of the SO's permanently open ocean or seasonal sea-ice zones (Figure S1 in Supporting Information S1). The CTG is comprised of diatoms with broad ecological affinities across marine, freshwater, and brackish environments. CTG diatoms have been found north of the polar front but are not recognized as regular components of Antarctic marine surface waters (Olguín & Alder, 2011; Olguin-Salinas et al., 2015; Pike et al., 2008). There is no evidence of CTG in-situ growth or any local populations.

AMTG and CTG diatom abundance time series exhibited contrasting features that broadly align with the total diatom abundance periods I and II. Changepoint analyses revealed major transitions during the 1960s, switching from higher (lower) relative abundance and variability of CTG (AMTG) between 1873 and 1964 (1873–1968), followed by a comparatively lower (higher) relative abundance and variability of CTG (AMTG) after 1965 (1969) (Figure 2c). During Period I, the AMTG represents 3.2% of the main diatom assemblage, while during the positive phase, it represents 62.1% (Period II) (Figure 2c).

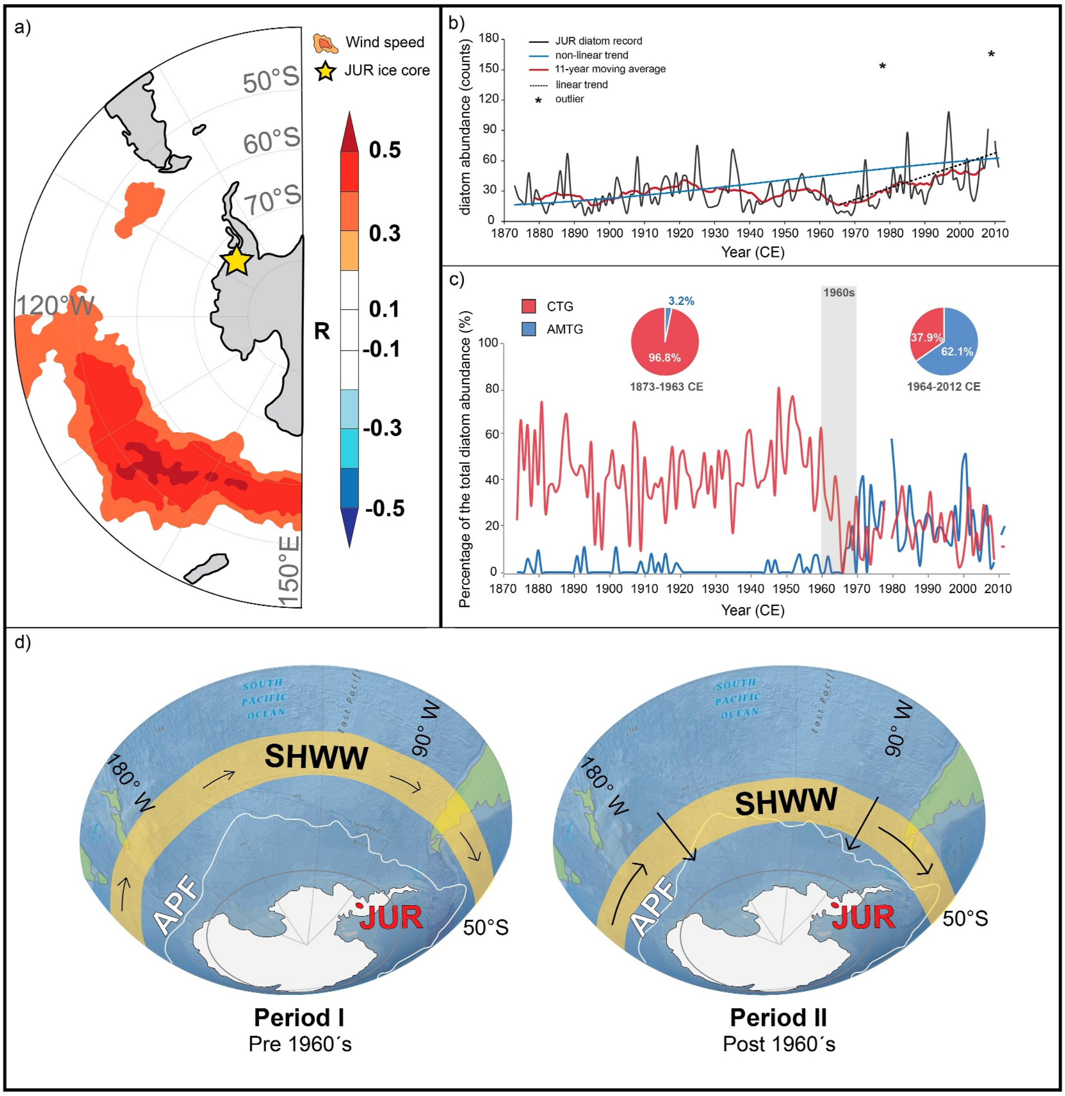

Figure 2. The Jurassic ice core diatom record (1873–2012 CE). (a) Regional map showing spatial correlations between the JUR annual diatom abundance record and ERA5 annual mean wind speed over the satellite-era. (b) Diatom abundance time series (black) overlayed by statistically significant ($p < 0.05$) non-linear trend (blue, see Section 2.3 for calculation), statistically significant ($p < 0.01$) linear trend during Period II (black dashed line) and 11-year moving average (red). The asterisk symbols in (b) denote the position and magnitude of outlier values removed from the data set. (c) Timeseries of Antarctic marine taxa group (AMTG) (blue line) and CTG (red line) relative contributions to the total annual diatom abundance record. Total annual diatom abundance percentage in (c) represents the contribution from unclassified diatoms (See Section 2.2; not shown in figure), AMTG and CTG. Pie charts in (c) represent the main diatom assemblage composition of the Jurassic ice core during Period I and Period II. Percentages reported in the pie charts were normalized to the main groups identified. Gray bar in (c) indicates the 1960s transition identified in the Jurassic ice core diatom record. (d) Schematic representing the inferred strengthening of the Pacific Southern Hemisphere Westerly Winds (SHWW) belt and its arrival to the Antarctic Surface Waters during Period II. Yellow shaded area in (d) represents the Pacific SHWW belt. APF = Antarctic Polar Front.

4. Discussion

4.1. Robust and Regional Wind Proxy

Diatom assemblage composition uniquely identifies the source region of diatoms preserved in ice core records (Allen et al., 2020; D. R. Tetzner, Allen, & Thomas, 2022; D. R. Tetzner, Thomas, et al., 2022). Diatom species in the AMTG are exclusively sourced from the pelagic SO (D. R. Tetzner, Allen, & Thomas, 2022). Whilst we acknowledge potential minor contributions from exposed diatom-bearing sediments (Barrett, 2013; McKay et al., 2008), the recovery of pristine fresh-looking diatoms from both groups, some still in colonies, suggests rapid transfer from modern water sources. Complementary previous airmass trajectory analyses (Figure S2 in Supporting Information S1) confirm the dominance of pathways across the Pacific sector of the SO to ice core sites in the AP (Allen et al., 2020; Thomas and Bracegirdle, 2009, 2015), supporting aeolian transport over the ocean (not landmasses) as the primary mechanism to rapidly transfer diatoms to the ice core site. Airmass trajectory findings are further complemented by previous Antarctic moisture source simulations which suggest moisture (and likely aerosols) reaching the JUR site is originated from the Pacific sector of the SO, in particular the open ocean region, south of 46°S and between 120 and 150°W (Gao et al., 2024). Furthermore, the strong spatial correlation between the diatom abundance and atmospheric circulation parameters draws a clear pathway for Pacific SHWW air parcels to be transported to the southern AP, supporting the effective southward transport of diatoms (Figure 2a). Thus, the Pacific sector of the SO is identified as the primary source of AMTG diatoms. This diatom diversity is a robust regional feature, identified in multiple ice cores across the Southern AP, exhibiting assemblages that are independent of local conditions (Allen et al., 2020; D. R. Tetzner, Allen, & Thomas, 2022). The representativity of the diatom abundance and diversity is supported by the presence of well-preserved AMTG diatom colonies and the constant proportion of fragments down-core, ruling out the possibility of progressive degradation biasing the magnitude of the diatom abundance.

4.2. Increasing Strength of SHWW Since the 1960s

The total annual diatom abundance is directly linked to changes in wind strength across the Pacific SHWW (Figure 2a), therefore, past changes in JUR diatom abundance can be used to reconstruct changes in wind strength over the Pacific SHWW. Prior to the 1960s (Period I), the Pacific SHWW were comparatively weaker than after the 1960s (Period II) (Figure 2b). The marked change in total diatom abundance from the 1960s onwards is interpreted as the onset of the recent intensification of SHWW in the Pacific sector. This transition is unprecedented over the last 140 years. The intensification of winds in the Pacific SHWW since the 1960s is consistent with the intensification of the Southern Hemisphere polar jet stream during the satellite-era (Goyal et al., 2021; Korhonen et al., 2010; Mayewski et al., 2013; Turner & Marshall, 2011; Young & Ribal, 2019) and direct observations of surface wind strengthening on Macquarie Island, at the westernmost end of the Pacific SHWW, since the mid-1960s (Adams, 2009; Saunders et al., 2018) (Figure 3c).

4.3. Southward Migration of the Pacific SHWW Since the 1960s

The enhanced relative abundance of AMTG during Period II (Figure 2c) indicates a strong interaction between the Pacific SHWW and the SO, with winds actively entraining diatoms from Antarctic Surface Waters. Conversely, the reduced relative abundance of AMTG during Period I indicates that the Pacific SHWW were not strongly interacting with Antarctic Surface Waters. Although we cannot ascribe a specific source region for the CTG, the divergence in the abundance patterns of the AMTG and CTG between periods I and II ratify that CTG diatoms were/are not sourced from Antarctic Surface Waters. Thus, we interpret the AMTG and CTG transitions during the 1960's as evidence for the poleward migration of the Pacific SHWW over Antarctic Surface Waters (Figure 2d). This poleward contraction is observed in the satellite record from 1979 onwards (Goyal et al., 2021; Korhonen et al., 2010; Mayewski et al., 2013; Turner & Marshall, 2011), and consistent with longer SAM reconstructions indicative of stable, weaker winds and a more equatorward position of the Pacific SHWW during the 19th century and the first half of the 20th century (Abram et al., 2014) (Figure 3b). However, our record uniquely identifies that the Pacific SHWW reached the SO as early as the 1960s, the first time this shift has occurred persistently in the past 140 years.

4.4. Significance of the 1960s Transition

Increased GHGs and ozone depletion have been identified as potential drivers of the recent observed changes in the SHWW (Arblaster & Meehl, 2006; Thompson et al., 2011; D. W. J. Thompson and Solomon, 2002; Wang et al., 2014). Both can amplify the upper tropospheric and stratospheric thermal gradient between Antarctica and the mid-latitudes, strengthening the polar vortex (Screen et al., 2018). Our results confirm that both the onset of the acceleration and the southward transition of the Pacific SHWW coincide with the abrupt decline in stratospheric ozone and the sustained increase in GHG since early-1960s (Masson-Delmotte et al., 2021; Shanklin, 2007) (Figure 3g). The timing of these events suggests that both GHG radiative forcing and ozone depletion may have driven the thermal imbalance in the atmosphere that led to the Pacific SHWW poleward strengthening.

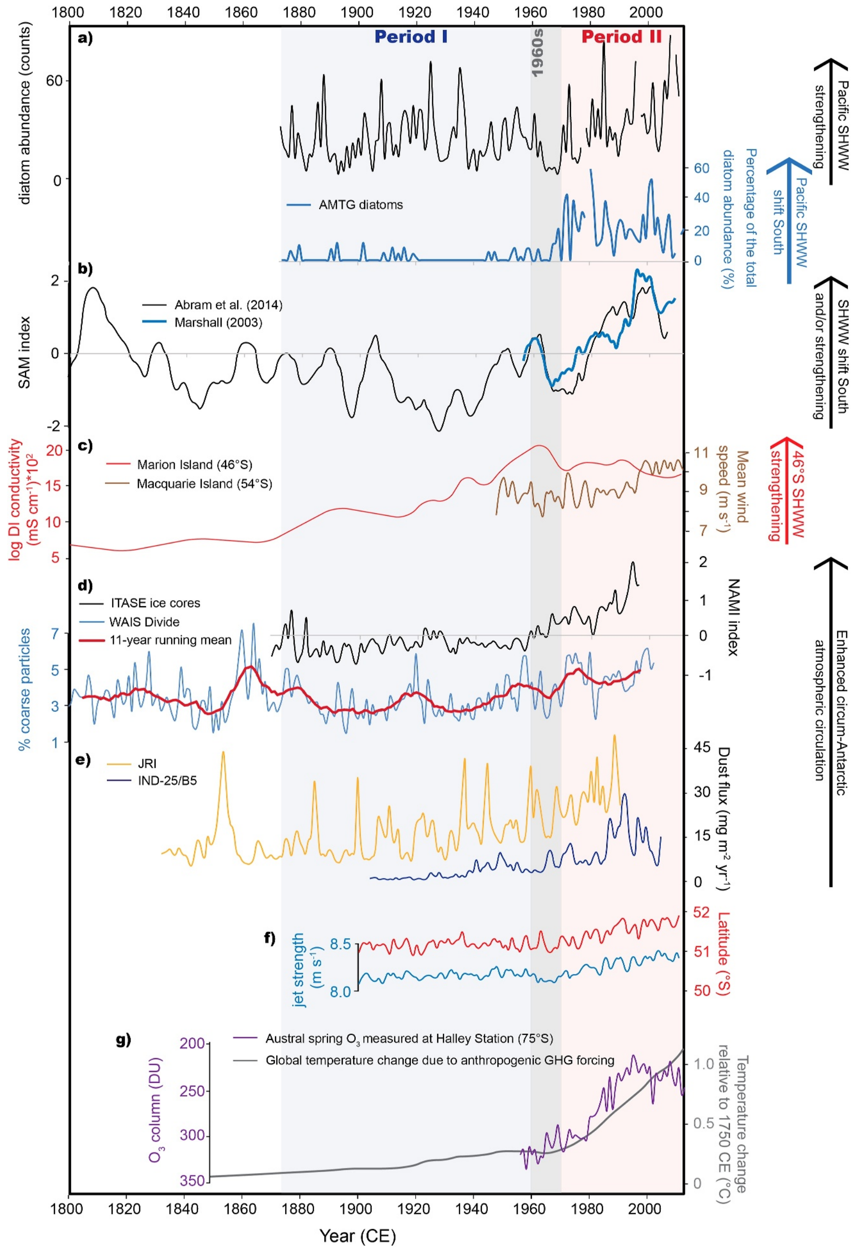

Figure 3. Comparison of the Jurassic ice core diatom record with multiple observed and reconstructed parameters. (a) JUR total annual diatom abundance record and Antarctic marine taxa group relative contribution to JUR's total annual diatom abundance record. (b) Southern Annular Mode (SAM) index obtained from meteorological observations (1958-present) (Marshall, 2003) and SAM index reconstructed from proxy records (1000 CE-present) (Abram et al., 2014). (c) Wind records from sub-Antarctic Islands. Inferred wind strength record (DI-conductivity) from Marion Island (46.9°S) (Perren et al., 2020) and annual wind speed measured at Macquarie Island (54°S) (Saunders et al., 2018). (d) Wind proxies from West Antarctic ice cores. Northerly Air Mass Incursions (NAMI) index from the International Trans-Antarctic Scientific Expedition ice cores (Dixon et al., 2012) and coarse particle percentage from the WAIS divide ice core (Koffman et al., 2014). (e) Wind proxies from ice cores in the Weddell sector. Dust flux from the James Ross Island ice core (McConnell et al., 2007) and from the IND-25/B5 ice core (Laluraj et al., 2020). (f) Position (inverted) and strength of maximum Southern Hemisphere surface westerly winds for CMIP6 models (Goyal et al., 2021). (g) Observed and reconstructed changes in atmospheric composition. The purple line indicates the total austral spring column ozone concentration (inverted) above Halley Station, Antarctica (Shanklin, 2007). The gray line shows the temperature change caused by total anthropogenic greenhouse gas forcing, relative to 1750 CE (Masson-Delmotte et al., 2021).

While GHG favored the atmospheric imbalance throughout the year, ozone depletion enhanced the effects during the austral summer (Fogt & Marshall, 2020; Thompson et al., 2011). Future climate change scenarios project a sustained poleward migration and strengthening of the SHWW, regardless of the expected stratospheric ozone recovery (Mayewski et al., 2015; Perlwitz et al., 2008). These projections highlight the greater importance of GHG on SHWW over the seasonal effects of ozone depletion in the future.

The recent strengthening and poleward migration of the Pacific SHWW have been shown to severely impact ice shelves along the Amundsen-Bellingshausen coast (Pritchard et al., 2012). The shift of the wind belt toward Antarctica increases the occurrence of foehn events that induce surface melting of the ice shelves (Cape et al., 2015; Turton et al., 2020), and enhance the upwelling of circumpolar deep water leading to basal melting of the ice shelves (Pritchard et al., 2012). These both promote ice shelf collapse, leading to the acceleration of glacier discharge, ultimately contributing to global mean sea-level rise (Pritchard et al., 2012). The strong relationship and rapid response of ice shelves to changing wind patterns (Cape et al., 2015; Turton et al., 2020), suggest the West Antarctic ice shelves could have been in a steady-state before the 1960s transition, with widespread thinning triggered after the early-1960s, in line with evidence from Pine Island Glacier (Smith et al., 2017). Identifying increased GHG emissions and ozone depletion among the main drivers of the Pacific SHWW transition and the abrupt response of the wind belt to these forcings provides key information to better understand the role SHWW have played in driving ice shelf instabilities and more accurately predict the fate of ice shelves under future climate change scenarios.

4.5. How Does This Fit With the Hemispheric Picture?

The recent intensification and poleward migration of the Pacific SHWW are coincident with changes observed in West Antarctic ice cores. The increasing trend in coarse particle percentage at WAIS (Koffman et al., 2014) and the shift to a positive phase of the Northerly Air Mass Incursions (NAMI) index (Dixon et al., 2012), both reflect a recent strengthening of the circum-Antarctic atmospheric circulation with greatest sensitivity to changes over the Pacific SHWW (Figure 3d). A poleward migration of the wind belt since the early-1960s is also interpreted from elevated conductivity in lake sediments from Marion Island, located in the Indian sector of the SO (Perren et al., 2020) (Figure 3c). In contrast, dust flux records from the Weddell Sea sector suggest an earlier enhancement in atmospheric circulation (Laluraj et al., 2020; McConnell et al., 2007) (∼1930s) (Figure 3e). The offset between these records (WAIS, International Trans-Antarctic Scientific Expedition and Marion Island vs. JRI and IND25/B5; Figure 3) could suggest a zonally asymmetric response of the SHWW (Fletcher & Moreno, 2012; Waugh et al., 2020), where the Atlantic sector of the SO reacted before the Pacific and the Indian sectors of the SO, or a strong dependence on source region conditions (e.g., South American aridity) on dust deposition, that is not related to winds (Bullard et al., 2016; Lambert et al., 2008; Wolff et al., 2010). Additionally, the recent poleward shift and strengthening of the Pacific SHWW validate results obtained from CMIP6 model runs (Goyal et al., 2021) (Figure 3f). Similarly, the long-term stability of winds prior to the 1960s is consistent with results obtained from data assimilation studies (Dalaiden et al., 2021; King et al., 2023; O'Connor et al., 2021).

5. Implications

The diatom record contained in the Jurassic ice core provides an unprecedented opportunity to track decadal changes in the location and strength of the Pacific SHWW beyond the instrumental period (1958-present). Results presented here will allow future attribution studies to constrain the behavior of the Pacific SHWW under future climate scenarios, in order to better predict the consequences of changes in Antarctic ice sheet mass balance and future sea level rise. Additionally, the extended wind record presented here can be used to determine the role that winds have played in driving environmental changes in the AP over the past 140 years, filling a major gap in our current understanding of regional climate change. The Jurassic ice core diatom record also demonstrates the exciting potential for other existing AP ice cores to yield valuable Pacific SHWW reconstructions over the last millennium.

Conflict of Interest

The authors declare no conflicts of interest relevant to this study.

Data Availability Statement

The data sets original to this work can be found in D. R. Tetzner, Allen, Thomas, Wolff, and Franzke (2025), published at the UK Polar Data Centre.

Acknowledgments

We would like to thank Shaun Miller, Emily Ludlow, and Sarah Jackson from the Ice Core Lab, British Antarctic Survey, for their help while cutting the ice and conducting the continuous flow analysis (CFA) in 2018. We would like to thank Iris Buisman and Giulio Lampronti from the Microscopy Lab, Earth Sciences Department, University of Cambridge, for their technical support in the use of the SEM. We want to thank the two anonymous reviewers for their constructive comments that led to an improved manuscript. This research was funded by CONICYT-Becas Chile and Cambridge Trust funding programme for PhD studies under Grant 72180432.

References

Abram, N. J., Mulvaney, R., Vimeux, F., Phipps, S. J., Turner, J., & England, M. H. (2014). Evolution of the southern annular mode during the past millennium. *Nature Climate Change*, *4*(7), 564–569. https://doi.org/10.1038/nclimate2235

Adams, N. (2009). Climate trends at Macquarie Island and expectations of future climate change in the sub-Antarctic. *Papers and Proceedings of the Royal Society of Tasmania*, *143*(1), 1–8. https://doi.org/10.26749/rstpp.143.1.1

Allen, C. S., Thomas, E. R., Blagbrough, H., Tetzner, D. R., Warren, R. A., Ludlow, E. C., & Bracegirdle, T. J. (2020). Preliminary evidence for the role played by South Westerly wind strength on the marine diatom content of an Antarctic Peninsula Ice Core (1980–2010). *Geosciences*, *10*(3), 87. https://doi.org/10.3390/geosciences10030087

Arblaster, J. M., & Meehl, G. A. (2006). Contributions of external forcings to southern annular mode trends. *Journal of Climate*, *19*(12), 2896–2905. https://doi.org/10.1175/jcli3774.1

Armand, L. K., Crosta, X., Romero, O., & Pichon, J. J. (2005). The biogeography of major diatom taxa in Southern Ocean sediments: 1. Sea ice related species. *Palaeogeography, Palaeoclimatology, Palaeoecology*, *223*(1–2), 66–92. https://doi.org/10.1016/j.palaeo.2005.03.028

Barrett, P. J. (2013). Resolving views on Antarctic Neogene glacial history—The Sirius debate. *Earth and Environmental Science Transactions of the Royal Society of Edinburgh*, *104*(1), 31–53. https://doi.org/10.1017/s175569101300008x

Browne, I. M., Moy, C. M., Riesselman, C. R., Neil, H. L., Curtin, L. G., Gorman, A. R., & Wilson, G. S. (2017). Late Holocene intensification of the westerly winds at the subantarctic Auckland Islands (51 S), New Zealand. *Climate of the Past*, *13*(10), 1301–1322. https://doi.org/10.5194/cp-13-1301-2017

Budgeon, A. L., Roberts, D., Gasparon, M., & Adams, N. (2012). Direct evidence of aeolian deposition of marine diatoms to an ice sheet. *Antarctic Science*, *24*(5), 527–535. https://doi.org/10.1017/s0954102012000235

Bullard, J. E., Baddock, M., Bradwell, T., Crusius, J., Darlington, E., Gaiero, D., et al. (2016). High-latitude dust in the Earth system. *Reviews of Geophysics*, *54*(2), 447–485. https://doi.org/10.1002/2016rg000518

Cape, M. R., Vernet, M., Skvarca, P., Marinsek, S., Scambos, T., & Domack, E. (2015). Foehn winds link climate-driven warming to ice shelf evolution in Antarctica. *Journal of Geophysical Research: Atmospheres*, *120*(21), 11–037. https://doi.org/10.1002/2015jd023465

Cefarelli, A. O., Ferrario, M. E., Almandoz, G. O., Atencio, A. G., Akselman, R., & Vernet, M. (2010). Diversity of the diatom genus Fragilariopsis in the Argentine sea and Antarctic waters: Morphology, distribution and abundance. *Polar Biology*, *33*(11), 1463–1484. https://doi.org/10.1007/s00300-010-0794-z

Cipriano, R. J., & Blanchard, D. C. (1981). Bubble and aerosol spectra produced by a laboratory breaking wave. *Journal of Geophysical Research*, *86*(C9), 8085–8092. https://doi.org/10.1029/jc086ic09p08085

Cole-Dai, J., Mosley-Thompson, E., & Thompson, L. G. (1997). Annually resolved southern hemisphere volcanic history from two Antarctic ice cores. *Journal of Geophysical Research*, *102*(D14), 16761–16771. https://doi.org/10.1029/97jd01394

Dalaiden, Q., Goosse, H., Rezsöhazy, J., & Thomas, E. R. (2021). Reconstructing atmospheric circulation and sea-ice extent in the West Antarctic over the past 200 years using data assimilation. *Climate Dynamics*, *57*(11), 3479–3503. https://doi.org/10.1007/s00382-021-05879-6

Dixon, D. A., Mayewski, P. A., Goodwin, I. D., Marshall, G. J., Freeman, R., Maasch, K. A., & Sneed, S. B. (2012). An ice-core proxy for northerly air mass incursions into West Antarctica. *International Journal of Climatology*, *32*(10), 1455–1465. https://doi.org/10.1002/joc.2371

Dutrieux, P., De Rydt, J., Jenkins, A., Holland, P. R., Ha, H. K., Lee, S. H., et al. (2014). Strong sensitivity of Pine Island ice-shelf melting to climatic variability. *Science*, *343*(6167), 174–178. https://doi.org/10.1126/science.1244341

Elster, J., Delmas, R. J., Petit, J.-R., & Řeháková, K. (2007). Composition of microbial communities in aerosol, snow and ice samples from remote glaciated areas (Antarctica, Alps, Andes). *Biogeosciences Discussions*, *4*, 1779–1813. https://doi.org/10.5194/bgd-4-1779-2007

Emanuelsson, B. D., Thomas, E. R., Tetzner, D. R., Humby, J. D., & Vladimirova, D. O. (2022). Ice core chronologies from the Antarctic Peninsula: The Palmer, Jurassic, and Rendezvous age-scales. *Geosciences*, *12*(2), 87. https://doi.org/10.3390/geosciences12020087

Farmer, D. M., McNeil, C. L., & Johnson, B. D. (1993). Evidence for the importance of bubbles in increasing air–sea gas flux. *Nature*, *361*(6413), 620–623. https://doi.org/10.1038/361620a0

Fletcher, M. S., & Moreno, P. I. (2012). Have the southern westerlies changed in a zonally symmetric manner over the last 14,000 years? A hemisphere-wide take on a controversial problem. *Quaternary International*, *253*, 32–46. https://doi.org/10.1016/j.quaint.2011.04.042

Fogt, R. L., & Marshall, G. J. (2020). The Southern annular mode: Variability, trends, and climate impacts across the Southern Hemisphere. *Wiley Interdisciplinary Reviews: Climate Change*, *11*(4), e652. https://doi.org/10.1002/wcc.652

Franzke, C. (2009). Multi-scale analysis of teleconnection indices: Climate noise and nonlinear trend analysis. *Nonlinear Processes in Geophysics*, *16*(1), 65–76. https://doi.org/10.5194/npg-16-65-2009

Franzke, C., OKane, T., Monselesan, D., Risbey, J., & Horenko, I. (2015). Systematic attribution of secular southern Hemispheric circulation trends with observational forcing data. *Nonlinear Processes in Geophysics*, *22*(5), 513–525. https://doi.org/10.5194/npg-22-513-2015

Gao, Q., Sime, L. C., McLaren, A. J., Bracegirdle, T. J., Capron, E., Rhodes, R. H., et al. (2024). Evaporative controls on Antarctic precipitation: An ECHAM6 model study using innovative water tracer diagnostics. *The Cryosphere*, *18*(2), 683–703. https://doi.org/10.5194/tc-18-683-2024

Gille, S. T. (2014). How ice shelves melt. *Science*, *346*(6214), 1180–1181. https://doi.org/10.1126/science.aaa0886

Goyal, R., Sen Gupta, A., Jucker, M., & England, M. H. (2021). Historical and projected changes in the Southern Hemisphere surface westerlies. *Geophysical Research Letters*, *48*(4), e2020GL090849. https://doi.org/10.1029/2020gl090849

Gruber, N., Landschützer, P., & Lovenduski, N. S. (2019). The variable Southern Ocean carbon sink. *Annual Review of Marine Science*, *11*(1), 159–186. https://doi.org/10.1146/annurev-marine-121916-063407

Harper, M. A., & McKay, R. M. (2010). Diatoms as markers of atmospheric transport. In E. F. Stoermer & J. P. Smol (Eds.), *The diatoms: Applications for the environmental and earth sciences* (pp. 552–559). Cambridge University Press. https://doi.org/10.1017/CBO9780511763175.032

Hasle, G. R., & Syvertsen, E. E. (1997). *Identifying marine phytoplankton*. Academic Press.

Hersbach, H., & Dee, D. (2016). ERA5 reanalysis is in production. *ECMWF Newsl*, *147*, 7.

Hinojosa, J. L., Moy, C. M., Stirling, C. H., Wilson, G. S., & Eglinton, T. I. (2017). A New Zealand perspective on centennial-scale Southern Hemisphere westerly wind shifts during the last two millennia. *Quaternary Science Reviews*, *172*, 32–43. https://doi.org/10.1016/j.quascirev.2017.07.016

Hosking, J. S., Orr, A., Marshall, G. J., Turner, J., & Phillips, T. (2013). The influence of the Amundsen–Bellingshausen Seas low on the climate of West Antarctica and its representation in coupled climate model simulations. *Journal of Climate*, *26*(17), 6633–6648. https://doi.org/10.1175/jcli-d-12-00813.1

Huang, N. E., Shen, Z., Long, S. R., Wu, M. C., Shih, H. H., Zheng, Q., et al. (1998). The empirical mode decomposition and the Hilbert spectrum for nonlinear and non-stationary time series analysis. *Proceedings of the Royal Society of London Series A: Mathematical, Physical and Engineering Sciences*, *454*(1971), 903–995. https://doi.org/10.1098/rspa.1998.0193

Huang, N. E., & Wu, Z. (2008). A review on Hilbert-Huang transform: Method and its applications to geophysical studies. *Reviews of Geophysics*, *46*(2), RG2006. https://doi.org/10.1029/2007rg000228

Killick, R., Fearnhead, P., & Eckley, I. A. (2012). Optimal detection of changepoints with a linear computational cost. *Journal of the American Statistical Association*, *107*(500), 1590–1598. https://doi.org/10.1080/01621459.2012.737745

King, J., Anchukaitis, K. J., Allen, K., Vance, T., & Hessl, A. (2023). Trends and variability in the southern annular mode over the common era. *Nature Communications*, *14*(1), 2324. https://doi.org/10.1038/s41467-023-37643-1

Koffman, B. G., Kreutz, K. J., Breton, D. J., Kane, E. J., Winski, D. A., Birkel, S. D., et al. (2014). Centennial-scale variability of the Southern Hemisphere westerly wind belt in the eastern Pacific over the past two millennia. *Climate of the Past*, *10*(3), 1125–1144. https://doi.org/10.5194/cp-10-1125-2014

Korhonen, H., Carslaw, K. S., Forster, P. M., Mikkonen, S., Gordon, N. D., & Kokkola, H. (2010). Aerosol climate feedback due to decadal increases in Southern Hemisphere wind speeds. *Geophysical Research Letters*, *37*(2), L02805. https://doi.org/10.1029/2009gl041320

Laluraj, C. M., Rahaman, W., Thamban, M., & Srivastava, R. (2020). Enhanced dust influx to south Atlantic sector of Antarctica during the late-20th century: Causes and contribution to radiative forcing. *Journal of Geophysical Research: Atmospheres*, *125*(8), e2019JD030675. https://doi.org/10.1029/2019jd030675

Lambert, F., Delmonte, B., Petit, J. R., Bigler, M., Kaufmann, P. R., Hutterli, M. A., et al. (2008). Dust-climate couplings over the past 800,000 years from the EPICA Dome C ice core. *Nature*, *452*(7187), 616–619. https://doi.org/10.1038/nature06763

Landschützer, P., Gruber, N., Haumann, F. A., Rödenbeck, C., Bakker, D. C., Van Heuven, S., et al. (2015). The reinvigoration of the Southern Ocean carbon sink. *Science*, *349*(6253), 1221–1224. https://doi.org/10.1126/science.aab2620

Le Quéré, C., Andrew, R. M., Friedlingstein, P., Sitch, S., Hauck, J., Pongratz, J., et al. (2018). Global carbon budget 2018. *Earth System Science Data*, *10*(4), 2141–2194. https://doi.org/10.5194/essd-10-2141-2018

Marshall, G. J. (2003). Trends in the southern annular mode from observations and reanalyses. *Journal of Climate*, *16*(24), 4134–4143. https://doi.org/10.1175/1520-0442(2003)016<4134:titsam>2.0.co;2

Masson-Delmotte, V., Zhai, P., Pirani, A., Connors, S. L., Péan, C., Berger, S., & Zhou, B. (2021). Climate change 2021: The physical science basis. Contribution of working group I to the sixth assessment report of the intergovernmental panel on climate change, *2*(1), 2391. https://doi.org/10.1017/9781009157896

MathWorks Inc. (2020). *MATLAB version: 9.9.0.1857802 (R2020b)*. The MathWorks Inc. Retrieved from https://www.mathworks.com

Mayewski, P. A., Bracegirdle, T., Goodwin, I., Schneider, D., Bertler, N. A. N., Birkel, S., et al. (2015). Potential for southern hemisphere climate surprises. *Journal of Quaternary Science*, *30*(5), 391–395. https://doi.org/10.1002/jqs.2794

Mayewski, P. A., Maasch, K. A., Dixon, D., Sneed, S. B., Oglesby, R., Korotkikh, E., et al. (2013). West Antarctica's sensitivity to natural and human-forced climate change over the Holocene. *Journal of Quaternary Science*, *28*(1), 40–48. https://doi.org/10.1002/jqs.2593

McConnell, J. R., Edwards, R., Kok, G. L., Flanner, M. G., Zender, C. S., Saltzman, E. S., et al. (2007). 20th-century industrial black carbon emissions altered arctic climate forcing. *Science*, *317*(5843), 1381–1384. https://doi.org/10.1126/science.1144856

McKay, R. M., Barrett, P. J., Harper, M. A., & Hannah, M. J. (2008). Atmospheric transport and concentration of diatoms in surficial and glacial sediments of the Allan Hills, Transantarctic Mountains. *Palaeogeography, Palaeoclimatology, Palaeoecology*, *260*(1–2), 168–183. https://doi.org/10.1016/j.palaeo.2007.08.014

Moreno, P. I., Vilanova, I., Villa-Martínez, R., Garreaud, R. D., Rojas, M., & De Pol-Holz, R. (2014). Southern annular mode-like changes in southwestern Patagonia at centennial timescales over the last three millennia. *Nature Communications*, *5*(1), 1–7.

Moy, C. M., Dunbar, R. B., Moreno, P. I., Francois, J. P., Villa-Martínez, R., Mucciarone, D. M., et al. (2008). Isotopic evidence for hydrologic change related to the westerlies in SW Patagonia, Chile, during the last millennium. *Quaternary Science Reviews*, *27*(13–14), 1335–1349. https://doi.org/10.1016/j.quascirev.2008.03.006

O'Connor, G. K., Steig, E. J., & Hakim, G. J. (2021). Strengthening southern hemisphere westerlies and Amundsen Sea low deepening over the 20th century revealed by proxy-data assimilation. *Geophysical Research Letters*, *48*(24), e2021GL095999. https://doi.org/10.1029/2021gl095999

Olguín, H. F., & Alder, V. A. (2011). Species composition and biogeography of diatoms in Antarctic and Subantarctic (Argentine shelf) waters (37–76 S). *Deep Sea Research Part II: Topical Studies in Oceanography*, *58*(1–2), 139–152. https://doi.org/10.1016/j.dsr2.2010.09.031

Olguín Salinas, H. F., Alder, V. A., Puig, A., & Boltovskoy, D. (2015). Latitudinal diversity patterns of diatoms in the Southwestern Atlantic and Antarctic waters. *Journal of Plankton Research*, *37*(4), 659–665. https://doi.org/10.1093/plankt/fbv042

Parkinson, C. L. (2019). A 40-y record reveals gradual Antarctic sea ice increases followed by decreases at rates far exceeding the rates seen in the Arctic. *Proceedings of the National Academy of Sciences*, *116*(29), 14414–14423. https://doi.org/10.1073/pnas.1906556116

Perlwitz, J., Pawson, S., Fogt, R. L., Nielsen, J. E., & Neff, W. D. (2008). Impact of stratospheric ozone hole recovery on Antarctic climate. *Geophysical Research Letters*, *35*(8), L08714. https://doi.org/10.1029/2008gl033317

Perren, B. B., Hodgson, D. A., Roberts, S. J., Sime, L., Van Nieuwenhuyze, W., Verleyen, E., & Vyverman, W. (2020). Southward migration of the Southern Hemisphere westerly winds corresponds with warming climate over centennial timescales. *Communications Earth & Environment*, *1*(1), 1–8. https://doi.org/10.1038/s43247-020-00059-6

Pike, J., Allen, C. S., Leventer, A., Stickley, C. E., & Pudsey, C. J. (2008). Comparison of contemporary and fossil diatom assemblages from the western Antarctic Peninsula shelf. *Marine Micropaleontology*, *67*(3–4), 274–287. https://doi.org/10.1016/j.marmicro.2008.02.001

Pritchard, H., Ligtenberg, S. R., Fricker, H. A., Vaughan, D. G., van den Broeke, M. R., & Padman, L. (2012). Antarctic ice-sheet loss driven by basal melting of ice shelves. *Nature*, *484*(7395), 502–505. https://doi.org/10.1038/nature10968

Saunders, K. M., Roberts, S. J., Perren, B., Butz, C., Sime, L., Davies, S., et al. (2018). Holocene dynamics of the Southern Hemisphere westerly winds and possible links to CO 2 outgassing. *Nature Geoscience*, *11*(9), 650–655. https://doi.org/10.1038/s41561-018-0186-5

Schimpf, D., Kilian, R., Kronz, A., Simon, K., Spötl, C., Wörner, G., et al. (2011). The significance of chemical, isotopic, and detrital components in three coeval stalagmites from the superhumid southernmost Andes (53 S) as high-resolution palaeo-climate proxies. *Quaternary Science Reviews*, *30*(3–4), 443–459. https://doi.org/10.1016/j.quascirev.2010.12.006

Screen, J. A., Bracegirdle, T. J., & Simmonds, I. J. C. C. R. (2018). Polar climate change as manifest in atmospheric circulation. *Current Climate Change Reports*, *4*, 383–395. https://doi.org/10.1007/s40641-018-0111-4

Shanklin, J. D. (2007). *BAS ozone data*. British Antarctic Survey. Retrieved from https://data.bas.ac.uk/fullrecord.php?id=GB/NERC/BAS/AEDC/00255

Shepherd, A., Ivins, E. R., Geruo, A., Barletta, V. R., Bentley, M. J., Bettadpur, S., et al. (2012). A reconciled estimate of ice-sheet mass balance. *Science*, *338*(6111), 1183–1189. https://doi.org/10.1126/science.1228102

Smith, J. A., Andersen, T. J., Shortt, M., Gaffney, A. M., Truffer, M., Stanton, T. P., et al. (2017). Sub-ice-shelf sediments record history of twentieth-century retreat of Pine Island Glacier. *Nature*, *541*(7635), 77–80. https://doi.org/10.1038/nature20136

Smol, J. & Stoermer, E. (Eds.) (2010). *The diatoms: Applications for the environmental and earth Sciences* (2nd ed.). Cambridge University Press. https://doi.org/10.1017/CBO9780511763175

Steig, E. J., Schneider, D. P., Rutherford, S. D., Mann, M. E., Comiso, J. C., & Shindell, D. T. (2009). Warming of the Antarctic ice-sheet surface since the 1957 international geophysical year. *Nature*, *457*(7228), 459–462. https://doi.org/10.1038/nature07669

Tetzner, D., Allen, C., Thomas, E., Wolff, E., & Franzke, C. (2025). Annual diatom abundance and diversity from the Jurassic ice core, Antarctic Peninsula (1873–2012 CE) (Version 1.0) [Dataset]. *NERC EDS UK Polar Data Centre*. https://doi.org/10.5285/371f680f-2c0b-4558-9a85-12aa8722be7e

Tetzner, D., Thomas, E. R., Allen, C. S., & Wolff, E. W. (2021). A refined method to analyze insoluble particulate matter in ice cores, and its application to diatom sampling in the Antarctic Peninsula. *Frontiers in Earth Science*, *9*, 617043. https://doi.org/10.3389/feart.2021.617043

Tetzner, D. R., Allen, C. S., & Thomas, E. R. (2022). Regional variability of diatoms in ice cores from the antarctic Peninsula and Ellsworth Land, Antarctica. *The Cryosphere*, *16*(3), 779–798. https://doi.org/10.5194/tc-16-779-2022

Tetzner, D. R., Allen, C. S., Thomas, E. R., & Humby, J. (2025). Use of excess meltwater from continuous flow analysis systems for the analysis of low concentration insoluble microparticles in ice cores. *Frontiers in Earth Science*, *13*, 1530875. https://doi.org/10.3389/feart.2025.1530875

Tetzner, D. R., Thomas, E. R., Allen, C. S., & Grieman, M. M. (2022). Regional validation of the use of diatoms in ice cores from the Antarctic Peninsula as a Southern Hemisphere westerly wind proxy. *Climate of the Past*, *18*(7), 1709–1727. https://doi.org/10.5194/cp-18-1709-2022

Thoma, M., Jenkins, A., Holland, D., & Jacobs, S. (2008). Modeling circumpolar deep water intrusions on the Amundsen Sea continental shelf, Antarctica. *Geophysical Research Letters*, *35*(18), L18602. https://doi.org/10.1029/2008gl034939

Thomas, E. R., & Bracegirdle, T. J. (2009). Improving ice core interpretation using in situ and reanalysis data. *Journal of Geophysical Research*, *114*(D20), D20116. https://doi.org/10.1029/2009jd012263

Thomas, E. R., & Bracegirdle, T. J. (2015). Precipitation pathways for five new ice core sites in Ellsworth Land, West Antarctica. *Climate Dynamics*, *44*(7–8), 2067–2078. https://doi.org/10.1007/s00382-014-2213-6

Thomas, E. R., Marshall, G. J., & McConnell, J. R. (2008). A doubling in snow accumulation in the western Antarctic Peninsula since 1850. *Geophysical Research Letters*, *35*(1), L01706. https://doi.org/10.1029/2007gl032529

Thompson, D. W., Solomon, S., Kushner, P. J., England, M. H., Grise, K. M., & Karoly, D. J. (2011). Signatures of the Antarctic ozone hole in Southern Hemisphere surface climate change. *Nature Geoscience*, *4*(11), 741–749. https://doi.org/10.1038/ngeo1296

Thompson, D. W. J., & Solomon, S. (2002). Interpretation of recent Southern Hemisphere climate change. *Science*, *296*(5569), 895–899. https://doi.org/10.1126/science.1069270

Turner, J., & Marshall, G. J. (2011). *Climate change in the polar regions*. Cambridge University Press.

Turner, J., Marshall, G. J., Clem, K., Colwell, S., Phillips, T., & Lu, H. (2020). Antarctic temperature variability and change from station data. *International Journal of Climatology*, *40*(6), 2986–3007. https://doi.org/10.1002/joc.6378

Turton, J. V., Kirchgaessner, A., Ross, A. N., King, J. C., & Kuipers Munneke, P. (2020). The influence of Föhn winds on annual and seasonal surface melt on the Larsen C Ice Shelf, Antarctica. *The Cryosphere*, *14*(11), 4165–4180. https://doi.org/10.5194/tc-14-4165-2020

Van Wessem, J. M., Ligtenberg, S. R. M., Reijmer, C. H., Van De Berg, W. J., Van Den Broeke, M. R., Barrand, N. E., et al. (2016). The modelled surface mass balance of the Antarctic Peninsula at 5.5 km horizontal resolution. *The Cryosphere*, *10*(1), 271–285. https://doi.org/10.5194/tc-10-271-2016

Vaughan, D. G. (2006). Recent trends in melting conditions on the Antarctic Peninsula and their implications for ice-sheet mass balance and sea level. *Arctic Antarctic and Alpine Research*, *38*(1), 147–152. https://doi.org/10.1657/1523-0430(2006)038[0147:rtimco]2.0.co;2

Waldmann, N., Ariztegui, D., Anselmetti, F. S., Austin Jr, J. A., Moy, C. M., Stern, C., et al. (2010). Holocene climatic fluctuations and positioning of the Southern Hemisphere westerlies in Tierra del Fuego (54 S), Patagonia. *Journal of Quaternary Science*, *25*(7), 1063–1075. https://doi.org/10.1002/jqs.1263

Wang, G., Cai, W., & Purich, A. (2014). Trends in Southern Hemisphere wind-driven circulation in CMIP5 models over the 21st century: Ozone recovery versus greenhouse forcing. *Journal of Geophysical Research: Oceans*, *119*(5), 2974–2986. https://doi.org/10.1002/2013jc009589

Warnock, J. P., & Scherer, R. P. (2015). A revised method for determining the absolute abundance of diatoms. *Journal of Paleolimnology*, *53*(1), 157–163. https://doi.org/10.1007/s10933-014-9808-0

Waugh, D. W., Banerjee, A., Fyfe, J. C., & Polvani, L. M. (2020). Contrasting recent trends in Southern Hemisphere Westerlies across different ocean basins. *Geophysical Research Letters*, *47*(18), e2020GL088890. https://doi.org/10.1029/2020gl088890

Wolff, E. W., Barbante, C., Becagli, S., Bigler, M., Boutron, C. F., Castellano, E., et al. (2010). Changes in environment over the last 800,000 years from chemical analysis of the EPICA Dome C ice core. *Quaternary Science Reviews*, *29*(1), 285–295. https://doi.org/10.1016/j.quascirev.2009.06.013

Xia, Z., Yu, Z., & Loisel, J. (2018). Centennial-scale dynamics of the southern hemisphere westerly winds across the Drake Passage over the past two millennia. *Geology*, *46*(10), 855–858. https://doi.org/10.1130/g40187.1

Young, I. R., & Ribal, A. (2019). Multiplatform evaluation of global trends in wind speed and wave height. *Science*, *364*(6440), 548–552. https://doi.org/10.1126/science.aav9527

Zielinski, U., & Gersonde, R. (1997). Diatom distribution in Southern Ocean surface sediments (Atlantic sector): Implications for paleoenvironmental reconstructions. *Palaeogeography, Palaeoclimatology, Palaeoecology*, *129*(3–4), 213–250. https://doi.org/10.1016/s0031-0182(96)00130-7

References From the Supporting Information

Allen, C. S., Pike, J., & Pudsey, C. J. (2011). Last glacial–interglacial sea-ice cover in the SW Atlantic and its potential role in global deglaciation. *Quaternary Science Reviews*, *30*(19–20), 2446–2458. https://doi.org/10.1016/j.quascirev.2011.04.002